Interpreting seasonal changes in the carbon balance of southern Amazonia using measurements of XCO_2 and chlorophyll fluorescence from GOSAT

Nicholas C. Parazoo,[1,2] Kevin Bowman,[1,2] Christian Frankenberg,[1] Jung-Eun Lee,[1] Joshua B. Fisher,[1] John Worden,[1] Dylan B. A. Jones,[2,3] Joseph Berry,[4] G. James Collatz,[5] Ian T. Baker,[6] Martin Jung,[7] Junjie Liu,[1] Gregory Osterman,[1] Chris O'Dell,[6] Athena Sparks,[1] Andre Butz,[8] Sandrine Guerlet,[9] Yukio Yoshida,[10] Huilin Chen,[11,12] and Christoph Gerbig[7]

Received 7 March 2013; revised 4 April 2013; accepted 5 April 2013; published 6 June 2013.

[1] Amazon forests exert a major influence on the global carbon cycle, but quantifying the impact is complicated by diverse landscapes and sparse data. Here we examine seasonal carbon balance in southern Amazonia using new measurements of column-averaged dry air mole fraction of CO_2 (XCO_2) and solar induced chlorophyll fluorescence (SIF) from the Greenhouse Gases Observing Satellite (GOSAT) from July 2009 to December 2010. SIF, which reflects gross primary production (GPP), is used to disentangle the photosynthetic component of land-atmosphere carbon exchange. We find that tropical transitional forests in southern Amazonia exhibit a pattern of low XCO_2 during the wet season and high XCO_2 in the dry season that is robust to retrieval methodology and with seasonal amplitude double that of cerrado ecosystems to the east (4 ppm versus 2 ppm), including enhanced dilution of 2.5 ppm in the wet season. Concomitant measurements of SIF, which are inversely correlated with XCO_2 in southern Amazonia ($r = -0.53$, $p < 0.001$), indicate that the enhanced variability is driven by seasonal changes in GPP due to coupling of strong vertical mixing with seasonal changes in underlying carbon exchange. This finding is supported by forward simulations of the Goddard Chemistry Transport Model (GEOS-Chem) which show that local carbon uptake in the wet season and loss in the dry season due to emissions by ecosystem respiration and biomass burning produces best agreement with observed XCO_2. We conclude that GOSAT provides critical measurements of carbon exchange in southern Amazonia, but more samples are needed to examine moist Amazon forests farther north. **Citation:** Parazoo, N. C., et al. (2013), Interpreting seasonal changes in the carbon balance of southern Amazonia using measurements of XCO_2 and chlorophyll fluorescence from GOSAT, *Geophys. Res. Lett.*, *40*, 2829–2833, doi:10.1002/grl.50452.

1. Introduction

[2] The Amazon basin plays a significant role in the global carbon cycle. Nearly half of all tropical biomass (120 Pg C) is stored in roots and trees, with 0.5 Pg C year^{-1} lost through deforestation and 0.6 Pg C year^{-1} gained by intact forests [*Malhi et al.*, 2009, and references therein]. There is also significant interannual variability in carbon exchange, driven by changes in the biophysical state of rain forests during large-scale disturbances such as drought, which cause anomalies in the global growth rate of atmospheric CO_2 [*Bousquet et al.*, 2000]. With vulnerability to drought stress expected to increase with climate change [e.g., *Phillips et al.*, 2009], Amazonian forests may play a more prominent role in modulating future increases of atmospheric CO_2 and, through radiative forcing, climate change [e.g., *Cox et al.*, 2004]. However, there is still much uncertainty in our understanding of basin-wide carbon balance.

[3] In particular, seasonal patterns of net ecosystem exchange (NEE) measured from flux towers vary significantly across Amazonia, with weak seasonal cycles in the north at Manaus, stronger seasonality to east at Tapajos National Forest near Santarem and south at Jarú Reserve and Fazenda Maracai (SIN), and still stronger seasonality southeast of Amazonia (e.g., Pe DeGigante) (sites described in *Keller et al.* [2004] and *Baker et al.*, [2013] and shown in Figure 1). These patterns predominantly follow vegetation and precipitation gradients [e.g., *da Rocha et al.*, 2009]; however, additional factors such as vegetation age, topography, and soil properties also influence NEE [e.g., *Keller et al.*, 2004]. Ecosystem models and flux tower measurements of gross primary production (GPP) and ecosystem

Additional supporting information may be found in the online version of this article.

[1]Jet Propulsion Laboratory, California Institute of Technology, Pasadena, California, USA.
[2]Joint Institute for Regional Earth System Science and Engineering, University of California, Los Angeles, California, USA.
[3]Department of Physics, University of Toronto, Toronto, Ontario, Canada.
[4]Department of Global Ecology, Carnegie Institution for Science, Stanford, California, USA.
[5]National Aeronautics' Space Administration, Goddard Space Flight Center, Greenbelt, Maryland, USA.
[6]Department of Atmospheric Science, Colorado State University, Fort Collins, Colorado, USA.
[7]Department for Biogeochemical Systems, Max Planck Institute for Biogeochemistry, Jena, Germany.
[8]IMK-ASF, Karlsruhe Institute of Technology, Leopoldshafen, Germany.
[9]Netherlands Institute for Space Research, Utrecht, Netherlands.
[10]Center for Global Environmental Research, National Institute for Environmental Studies, Tsukuba, Japan.
[11]NOAA Earth System Research Laboratory, Boulder, Colorado, USA.
[12]Now at Center for Isotope Research, University of Groningen, Groningen, The Netherlands.

Corresponding author: N. Parazoo, Jet Propulsion Laboratory, California Institute of Technology, Pasadena, CA 91109, USA. (Nicholas.C.Parazoo@jpl.nasa.gov)

0094-8276/13/10.1002/grl.50452

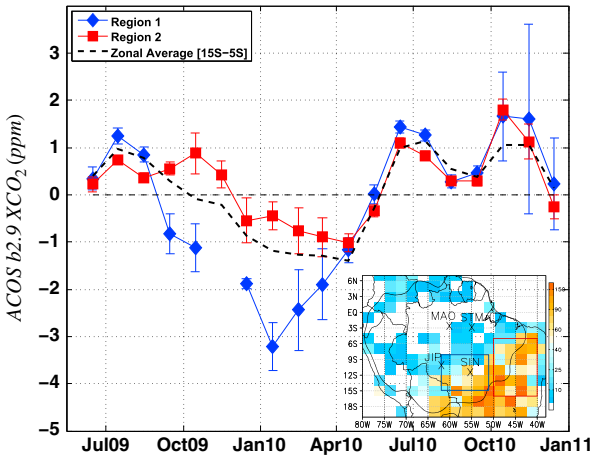

Figure 1. Seasonal cycle of ACOS b2.9 XCO_2 in southern Amazonia (blue, region 1), southeastern Amazonia (red, region 2), and southern Hemisphere tropics ([15°S–5°N, 180°W–180°E], land points only). We use a minimum of three samples to calculate monthly means. Uncertainty is estimated as the standard monthly error. Secular trend (black dashed) based on CO_2 data from Mauna Loa and South Pole Station (http://www.esrl.noaa.gov/gmd/ccgg/trends/) is removed. The map inset shows the total number of samples per 2.5° × 2° grid box from July 2009 to December 2010, contours of Amazonia (black) and eco-regions (blue and red), and locations of flux tower sites.

respiration have contributed greatly to our physiological understanding of seasonal carbon balance in Amazonia, but progress has been hindered by the limited spatial coverage and local nature of flux tower data.

[4] Advancing our understanding of the seasonal carbon balance requires a network for monitoring carbon fluxes at ecosystem scale. Measurements of atmospheric CO_2 provide such a constraint on NEE [*Bousquet et al.*, 2000]. For example, aircraft measurements in eastern Amazonia help to quantify the underlying seasonal carbon balance, but only for eastern Amazonia [*Gatti et al.*, 2010]. Dedicated measurements from new spaceborne instruments offer the potential to substantially improve sampling of Amazonia. The Greenhouse gasses Observing SATellite (GOSAT) has produced global retrievals of column-averaged dry air mole fraction of CO_2 (XCO_2) since June 2009 [*Watanabe et al.*, 2010]. Ground based evaluation of XCO_2 has relied primarily on the Total Carbon Column Observing Network (TCCON). Although GOSAT XCO_2 has high noise, in general, there is good seasonal agreement at northern latitude sites and during dry season months at the tropical site in Darwin, Australia [*Butz et al.*, 2011; *Wunch et al.*, 2011].

[5] Concurrent measurements of solar induced chlorophyll fluorescence (SIF) from GOSAT offer the potential to provide regional-scale constraints on GPP [*Frankenberg et al.*, 2011a; *Joiner et al.*, 2011] to better understand drivers of NEE variability. SIF is light re-emitted from chlorophyll receptors during photosynthesis and therefore offers a direct probe into the photosynthetic process [*Damm et al.*, 2010]. Retrievals of SIF from GOSAT correlate strongly ($r^2 = 0.80$) with ecosystem-scale GPP from the Max-Planck-Institute for Biogeochemistry (MPI-BGC) GPP model model [*Frankenberg et al.*, 2011b], indicating that, on average, most of the photosynthesis that occurs during emissions of SIF also leads to carbon assimilation. It therefore appears that SIF has skill in detecting large-scale GPP changes, including the physiological effects of drought [e.g., *Daumard et al.*, 2010].

[6] While GOSAT represents a major improvement in the number of CO_2 observations in the lower tropical atmosphere, most soundings in the tropics are unusable due to the presence of clouds and aerosols [*Crisp et al.*, 2012]. Consequently, data of the highest quality and quantity are located in southern portions of tropical South America, including transitional tropical forests in southern Amazonia and cerrado ecosystems to the southeast (map inset in Figure 1). According to *Davidson et al.* [2012], these regions are uniquely different in terms of total annual precipitation and vegetation type. In general, region 1 is wetter and has a much larger fraction of tropical evergreen forest than region 2 to the east, which is predominantly cerrado. We therefore examine seasonal carbon balance in these unique but poorly sampled eco-regions through joint analysis of XCO_2 and SIF data from GOSAT. There are three main objectives: (1) quantify and evaluate robustness of seasonal XCO_2 variations across tropical eco-regions, (2) relate XCO_2 variability to underlying biology, and (3) examine the photosynthetic component of biological carbon exchange using SIF.

2. Methods

[7] Retrievals of XCO_2 are calculated from the NASA Atmospheric CO_2 Observations from Space Build 2.9 (ACOS b2.9) algorithm [*O'Dell et al.*, 2012]. These data reproduce much of the expected global spatial and seasonal patterns of XCO_2, including negligible global bias (~0.13 ppm) and ~30% reduction in variance compared to previous versions [*Osterman et al.*, 2011; *Crisp et al.*, 2012]. ACOS b2.9 is corrected a posteriori for errors related to instrumental, observational, and geophysical parameters [*Wunch et al.*, 2011]. To evaluate XCO_2 retrievals in Amazonia, we compare ACOS b2.9 to estimates from ACOS Build 2.10 (ACOS b2.10), RemoTeC (SRON-Netherlands Institute for Space Research/KIT-Karlsruhe Institute of Technology) [*Butz et al.*, 2011], and NIES SWIR L2 V02 (NIES) [*Yoshida et al.*, 2011]. See auxiliary material for quality control procedures.

[8] Two steps are taken to relate XCO_2 variability in Amazonia to underlying biological processes. First, we compare XCO_2 to estimates of GPP from SIF (see below) to assess the empirical relationship between XCO_2 and underlying biology. Second, we run transport simulations in which a wide range of NEE estimates are used to drive the GEOS-Chem global transport model (see *Nassar et al.* [2010] for details). Model output is then compared to GOSAT XCO_2. By accounting for long-range transport, we can assess which pattern of NEE is most consistent with observations.

[9] Details of SIF, including retrieval, methods, and sampling biases are given in SI. SIF is retrieved following *Frankenberg et al.* [2011a]. We estimate changes in GPP by scaling SIF using the slope of linear fit between SIF and model GPP in the global and annual average. Midday retrievals are converted to daily averages by scaling SIF by the cosine of the solar zenith angle, then aggregated to 2.5° × 2°. Although the R^2 of model GPP and SIF ranges from 0.63 in Simple Biosphere Model, version 3, 0.67 in Carnegie-Ames-Stanford Approach-Global Fire Emissions Database version 3, and

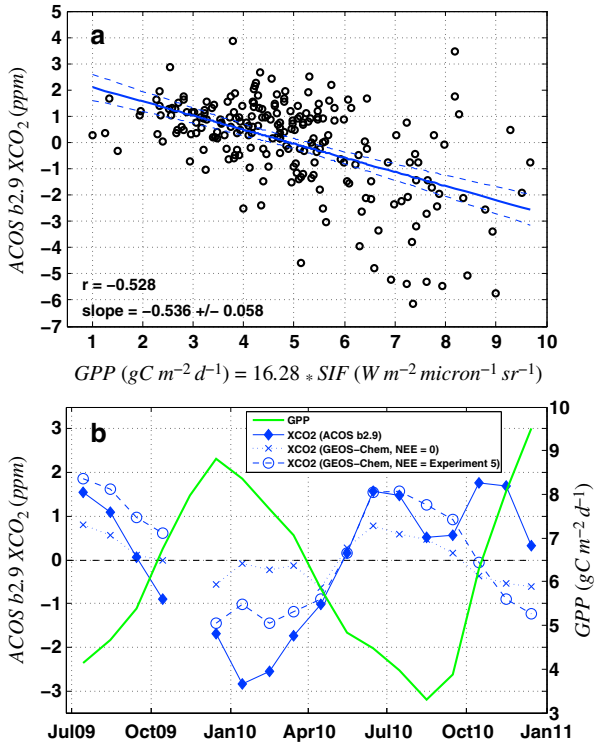

Figure 2. (a) Scatter plot of 2.5° × 2° grid cell monthly mean XCO_2 versus gross primary production (GPP) in southern Amazonia. GPP is approximated as SIF * m, where m = 16.28 is the linear fit between MPI GPP and chlorophyll fluorescence. Linear regression lines in solid blue and 95% confidence interval in dashed blue. Linear Pearson correlation (r) and slope/SE of regression are also shown. (b) Comparison of XCO_2 (blue solid, same as Figure 1) in region 1 to XCO_2 output from GEOS-Chem using NEE from the control experiment (blue dotted) and Experiment 5 (blue dashed, NEE experiments described in Table 1). Seasonal GPP from Figure 2a is plotted in green.

0.83 in MPI, we find this technique gives estimates of seasonal change in GPP in Amazonia that is robust to the choice of calibration model and with reduced variance relative to models.

[10] Despite the potential of satellite measurements of SIF to deliver globally distributed information on GPP, we stress that SIF methods are still new, challenging, and uncertain. In particular, we assume GPP scales with SIF by the same linear factor at global scale. Furthermore, we are limited to clear sky snapshots, which leads to under sampling of thick clouds and smoky skies. This sampling bias may cause differences in observed and expected time averaged GPP due to sensitivity to total incoming radiation. Given these limitations, GPP is treated more as a correlative measure rather than an absolute estimate (i.e., the technique is better suited to address changes in GPP than absolute values).

3. Results

[11] Seasonal XCO_2 over Amazon eco-regions is plotted in Figure 1. XCO_2 in tropical transitional forests (blue box, region 1) is plotted in blue; XCO_2 in cerrado ecosystems (red box, region 2) is plotted in red. XCO_2 has a similar seasonal phase in these regions, with highest mixing ratios in the dry season (~June–August) and lowest mixing ratios in the wet season (~November–February). However, the amplitude is twice as strong in region 1 (4 ppm compared to 2 ppm). Regional differences are most pronounced from September 2009 through March 2010, including the end of the dry season and most of the wet season, with XCO_2 in region 1 diluted by up to 2.5 ppm relative to region 2.

[12] With the exception of October and November 2010, these seasonal signals appear to be robust to measurement error. In particular, the seasonal amplitudes of regions 1 and 2 exceed the standard monthly error (≤1.0 ppm and 0.5 ppm, respectively), indicating the seasonal signal is statistically significant relative to monthly variability. In addition, regional signals, including difference between regions of 2.5 ppm during the 2009–2010 wet season, are robust to retrieval methodology, bias correction technique, quality control criteria, and specific soundings used (Figure S2).

[13] The role of non-local processes such as long-range transport on XCO_2 variability in southern Amazonia is also examined in Figure 1. We find that seasonal variations in region 2 tend to track changes in the Southern Hemisphere tropical zonal average to within 1 ppm for the entire period of record. This indicates that transport of background CO_2 has a strong influence on column variations in region 2. The same is generally true for region 1 during dry season and transitional months, suggesting background CO_2 also has a strong influence on the continental interior; however, XCO_2 is lower by 1–2 ppm from September 2009 to March 2010, indicating local processes contribute substantial variability in southern Amazonia during the wet season.

[14] Comparison of clear sky XCO_2 with SIF provides evidence that these local effects have biological origin. Figure 2a shows that XCO_2 is inversely correlated with SIF, and hence GPP, in region 1, with high XCO_2 corresponding to low GPP (and vice versa). Furthermore, XCO_2 is better correlated with GPP in region 1 (Figure 2a, $r = -0.53$, $p < 0.001$) than in region 2 ($r = -0.34$, not shown), and twice as sensitive to changes in GPP in region 1 (slope = -0.54 ± 0.06 ppm/g C m^{-2} d^{-1} and -0.26 ± 0.04 ppm/g C m^{-2} d^{-1}, respectively). The pattern for higher slope and correlation in region 1 is robust to retrieval product and bias correction technique except for NIES (Figure S2 and Table S1), which excludes most wet season data due to strict quality control. Seasonal plots of GPP and XCO_2 (Figure 2b) show the inverse relationship is strongest through July 2010, after which GPP and XCO_2 increase together. The correlation improves slightly ($r = -0.59$) when months after July 2010 are ignored, suggesting another mechanism becomes dominant at this time.

[15] Sensitivity of XCO_2 to local surface processes requires a combination of ecophysiology and dynamical effects. In particular, NEE must be coupled locally with strong vertical mixing. *Keppel-Aleks et al.* [2011] show this latter condition is not satisfied in high northern latitudes due to the nature of the atmospheric circulation, which favors horizontal advection, causing non-local effects to dominate column variations. Trace gases in the tropical atmosphere, however, are generally well mixed by deep and persistent cumulus convection [e.g., *Denning et al.*, 1999]. Consequently, variations in CO_2 forced at the surface by local carbon fluxes are rapidly mixed into the column.

Table 1. Results From Net Ecosystem Exchange (NEE) Sensitivity Experiments[a]

Scenarios for Seasonal Carbon Exchange (NEE = 1.7 g C m^{-2} d^{-1})			XCO_2 Comparison (GEOS-Chem Versus ACOS b2.9)	
Experiment Name	Wet Season NEE (Nov–Feb)	Dry Season NEE (Jun–Sep)	r	Slope
Control	Steady State	Steady State	0.43	1.41 ± 0.77 (fail)
1	Source	Steady State	−0.31	-1.09 ± 0.86 (fail)
2	Sink	Steady State	0.61	1.14 ± 0.38 (pass)
3	Steady State	Source	0.55	1.01 ± 0.40 (pass)
4	Steady State	Sink	−0.20	-1.14 ± 1.39 (fail)
5	Sink	Source	0.63	0.81 ± 0.26 (pass)
6	Source	Sink	−0.65	-1.68 ± 0.50 (fail)
7	Source	Source	0.26	0.81 ± 0.77 (fail)
8	Sink	Sink	0.48	1.53 ± 0.73 (fail)

[a]NEE scenarios (column 1) are based on the sign of seasonal carbon exchange during the wet (Nov-Mar) and dry (Jun-Sep) season (column 2 and 3, respectively), where source represents a flux to the atmosphere (and vice versa).

Model XCO_2 is calculated by running non-NEE CO_2 fluxes as described in *Nassar et al*. [2010] and each NEE scenario through GEOS-Chem, sampling output at ACOS b2.9 soundings, and converting to XCO_2 using the ACOS averaging kernel. XCO_2 is then aggregated over region 1, averaged at monthly timescales, and detrended as in Figure 1. Linear Pearson correlation coefficient (r) and slope of regression with 95% confidence interval (slope) are shown in columns 4 and 5, respectively, with results of Student's t-test on slope = 0 in parenthesis. Slopes greater than one indicate seasonal amplitude is underestimated (and vice versa).

[16] We use GEOS-Chem to test this claim; and in addition, help quantify seasonal carbon balance in region 1. We first test the null hypothesis that long-range transport explains XCO_2 variability in region 1. In this control experiment, we prescribe global NEE, biomass burning, air-sea gas exchange, and fossil fuel following *Nassar et al*. [2010] but set carbon fluxes within tropical South America (all grid points north of 20°S) to zero. Seasonal XCO_2 output from GEOS-Chem is weakly correlated with observations in region 1 ($r = 0.43$, see Table 1), the slope of regression is not significant from zero (slope = 1.41 ± 0.77), and seasonal amplitude is strongly damped relative to observations (1 ppm versus 4 ppm, Figure 2b), with a model excess of 2–3 ppm in the wet season and deficit of 1 ppm in the dry season. In contrast, GEOS-Chem is correlated with observations in region 2 ($r = 0.60$), with significant slope (1.172 ± 0.39) and most of the seasonal amplitude reproduced (1.5 ppm versus 2 ppm, not shown). These results suggest that transport dominates variability in region 2 but has a much weaker influence in region 1.

[17] In order to explain XCO_2 variability in region 1, we postulate that wet season carbon uptake and dry season efflux such as that reported from 3 years of flux tower data at Fazenda Maracai (SIN in Figure 1), a mature Brazilian transitional tropical forest site in the center of region 1 [*Vourlitis et al*., 2004], are needed. We test this hypothesis using the same model setup as before except steady state NEE in region 1 is replaced with estimates of seasonal NEE reported in the literature. These estimates range from strongly seasonal, including wet season source and/or dry season sink and reversed patterns, to weakly seasonal, including year round source, steady state, and sink [*Keller et al*., 2004; *Stephens et al*., 2007; *Baker et al*., 2013]. We test a total of eight scenarios for NEE (Table 1), assuming a constant flux of 1.7 g C m^{-2} d^{-1} (or 500 kg C ha^{-1} mo^{-1}, representing average minimum and maximum NEE at the four sites reported by *Keller et al*., [2004]) and that wet and dry seasons are either a source, sink, or in steady state.

[18] Correlation and slope of regression between observed and model XCO_2 are shown in Table 1. In half the cases (Experiments 1, 4, 6, and 7), the correlation decreases relative to the control run and linear regression fails the Student's t-test on slope = 0, with the seasonal cycle reversed relative to observations when a wet season source and/or dry season sink is assumed (1, 4, and 7). The best correlations emerge when a wet season sink and/or dry season source is assumed (2, 3, and 5, $r = 0.6$, 0.55, and 0.63, respectively) with slopes significant from zero and close to 1 (1.14 ± 0.38, 1.01 ± 0.40, and 0.83 ± 0.26). A visual comparison of observed and model variability (Figure 2b) shows our hypothesis of wet season uptake and dry season efflux (Experiment 5) is valid from July 2009 to August 2010 but is violated in October and November 2010, at which time observed XCO_2 increases but model XCO_2 decreases. Experiment 5 provides a much improved fit when these months are ignored ($r = 0.93$ and slope = 1.11 ± 0.12).

[19] We postulate that seasonal NEE driven by GPP is the primary source of XCO_2 variability through the middle of the 2010 dry season but that biomass burning in southeast Amazonia is the primary source of enhanced XCO_2 at the end of the 2010 dry season. *Marengo et al*. [2008] show that most drought years have increased forest fires due to extended periods of anomalously dry conditions. A major drought persisted through much of southern Amazonia in 2010, causing enhanced water stress throughout the dry season [e.g., *Lewis et al*., 2011; *Lee et al*., in review]. Measurements of Pollution in the Troposphere data show enhanced carbon monoxide in Amazonia (relative to the background) from August to October 2010 (see Figure S8), indicating a biomass burning source. Finally, *Chen et al*. [2011] use MODIS active fire data to show the presence of forest fires in southeastern Amazonia. It is therefore likely that biomass burning explains high XCO_2 in October and November 2010, which occurs in regions 1 and 2 and in all retrieval products (Figure S2). In addition, we attribute high XCO_2 variance in region 1 to transport from region 2 and reduced sampling coverage due to high aerosol loading (three samples in October 2010 versus 15 in October 2009).

4. Discussion and Conclusions

[20] We observe a distinct seasonal cycle in XCO_2 in southern Amazonia in clear sky conditions, with low mixing ratios in the wet season and high mixing ratios in the dry season. The seasonal phase resembles cerrado ecosystems to the east but the amplitude is twice as strong (4 ppm versus 2 ppm) due to the combination of deep vertical mixing with strongly seasonal GPP, creating local carbon imbalance with respiration. After accounting for the effects of long-range transport in GEOS-Chem, our results suggest that carbon is gained in southern Amazonia during the wet season and lost in the dry season. These findings are consistent with GPP and NEE measurements at Fazenda Maracai and Jaru. As this is a transitional forest with an extended dry season, it is likely that water limitation effects, including exacerbation of water stress during the 2010 drought, drive variations of GPP and NEE. Finally, we provide evidence that strong biomass burning during the 2010 drought contributes to enhanced XCO_2 at the end of the 2010 dry season.

[21] Without an extended record of data, however, the effect of seasonal and interannual variability is unclear. Additionally, the limited spatial coverage of GOSAT prevents examination of carbon dynamics in moist forests in northern Amazonia. Land surface models and flux tower measurements indicate much spatial heterogeneity in the Amazon carbon cycle due to strong gradients in annual precipitation, dry season length, and vegetation type. Because of this spatial and temporal variability, estimates of carbon exchange at annual and continental scales are unlikely to substantially improve our understanding of the role of Amazonia in the global carbon cycle. However, we are optimistic that disentangling seasonal and interannual effects will be possible over the next few years as the GOSAT record expands and additional dedicated CO_2 satellites such as the NASA OCO-2 become available. In addition, OCO-2 will have a much smaller footprint (~4 km), which will help see through clouds, and several orders of magnitude more measurements, which together should improve sampling of Amazonia.

[22] We use an ensemble approach to demonstrate robustness of the results to details of the XCO_2 retrieval algorithm, but we note these efforts do not constitute validation. Furthermore, there is significant scatter in XCO_2, and because systematic sampling of clear sky conditions may introduce sampling biases exceeding 1 ppm (e.g., *Corbin et al*. [2008] and Figure S3), further examination of cloudy sky data is needed. Such problems should be alleviated by OCO-2. In addition, a TCCON site will be installed at Manaus in northern Amazonia in November 2013, which will greatly improve evaluation of tropical data. Despite these issues, it is encouraging to see that satellite XCO_2 is sensitive to local processes in southern Amazonia and potentially constrains estimates of land-atmosphere CO_2 exchange in this critical region.

[23] **Acknowledgments.** ACOS b2.9 XCO_2 data were produced by the ACOS/OCO-2 project at the Jet Propulsion Laboratory, CalTech, and obtained from the ACOS/OCO-2 data archive maintained at the NASA GES DISC. Development of RemoTeC algorithm is partly funded from ESA's CCI on GHGs and the European Commission's seventh framework program under grant agreement 218793 and by the Emmy-Noether programme of DFG through grant BU2599/1-1. CarbonTracker 2011 results provided by NOAA ESRL, Boulder, Colorado, USA from the website at http://carbontracker.noaa.gov. We thank Prof. Dr. Paulo Artaxo, Dr. Kenia Wiedemann, Fernando Morais, Alcides Ribeiro, University of Sao Paulo, Brazil, and Livia Oliveira, INPA, Brazil, for their assistance and support in installing and operating the Picarro instrument at the TT34 tower. Part of this research was carried out at the Jet Propulsion Laboratory, California Institute of Technology, under a contract with NASA © 2013. All rights reserved.

[24] The Editor thanks an anonymous reviewer for his/her assistance in evaluating this paper.

References

Baker, I. T., et al. (2013), Surface ecophysiological behavior across vegetation and moisture gradients in tropical South America, *Agric. Forest Meteorol.*, http://dx.doi.org/10.1016/j.agrformet.2012.11.015.

Bousquet, P., P. Peylin, P. Ciais, C. Le Quere, P. Friedlingstein, and P. P. Tans (2000), Regional changes in carbon dioxide fluxes of land and oceans since 1980, *Science*, *290*, 1342, doi:10.1126/science.290.5495.1342.

Butz, A., et al. (2011), Toward accurate CO2 and CH4 observations from GOSAT, *Geophys. Res. Lett.*, *38*, L14812, doi:10.1029/2011GL047888.

Chen, Y., J. T. Randerson, D. C. Morton, R. S. DeFries, G. J. Collatz, P. S. Kasibhatla, L. Giglio, Y. Jin, and M. E. Marlier (2011), Forecasting fire season severity in South America using seas surface temperature anomalies, *Science*, *334*, 787–91, doi:10.1126/science.1209472.

Corbin, K. D., A. S. Denning, L. Lu, J.-W. Wang, and I. T. Baker (2008), Possible representation errors in inversions of satellite CO2 retrievals, *J. Geophys. Res.*, *113*(D2), D02301, doi:10.1029/2007JD008716.

Cox, P. M., R. A. Betts, M. Collins, P. P. Harris, C. Huntingford, and C. D. Jones (2004), Amazonian forest dieback under climate-carbon cycle projections for the 21st century, *Theor. Appl. Climatol.*, *78*, 137–156, doi:10.1007/s00704-004-0049-4.

Crisp, D., et al. (2012), The ACOS CO2 retrievals algorithm - Part II: Global XCO2 data characterization, *Atmos. Meas. Tech.*, *5*, 687–707.

da Rocha, H. R., et al. (2009), Patterns of water and heat flux across a biome gradient from tropical forest to savanna in Brazil, *J. Geopyhs. Res.*, *114*(G1), G00B12, doi:10.1029/2007JG000640.

Damm, A., et al. (2010), Remote sensing of sun-induced fluorescence to improve modeling of diurnal courses of gross primary production (GPP), *Global Change Biol.*, *16*, 171–186.

Daumard, F., S. Champagne, A. Fournier, Y. Goulas, A. Ounis, J.-F. Hanocq, and I. Moya (2010), A field platform for continuous measurement of canopy fluorescence, *IEEE T. Geosci. Remote*, *48*, 3358.

Davidson, E. A., et al. (2012), The Amazon basin in transition, *Nature*, *481*, doi:10.1038/nature10717.

Denning, A. S., et al. (1999), Three-dimensional transport and concentration of SF6: A model intercomparisons study (TransCom 2), *Tellus*, *51B*, 266–297.

Frankenberg, C., A. Butz, and G. C. Toon (2011a), Disentangling chlorophyll fluorescence from atmospheric scattering effects in O2 A-band spectra of reflected sun-light, *Geophys. Res. Lett.*, *38*, L03801, doi:10.1029/2010GL045896.

Frankenberg, C., et al. (2011b), New global observations of the terrestrial carbon cycle from GOSAT: Patterns of plant fluorescence with gross primary productivity, *Geophys. Res. Lett.*, *38*, L17706, doi:10.1029/2011GL048738.

Gatti, L. V., J. B. Miller, M. T. S. D'Amelio, A. Martinewski, L. S. Basso, M. E. Gloor, S. Wofsy, and P. Tans (2010), Vertical profiles of CO_2 above eastern Amazonia suggest a net carbon flux to the atmosphere and balanced biosphere between 2000 and 2009, *Tellus B*, *5*, 582–594.

Joiner, J. Y., Y. Yoshida, A. P. Vasilkov, Y. Yoshida, L. A. Corp, and E. M. Middleton (2011), First observations of global and seasonal terrestrial chlorophyll fluorescence from space, *Biogeosciences*, *8*, 637–651, doi:10.5194/bg-8-637-2011.

Keller, M., et al. (2004), Ecological research in the large-scale biosphere-atmosphere experiment in Amazonia: Early results, *Ecol. Appl.*, *14*(4), supplement, S3–S16.

Keppel-Aleks, G., P. O. Wennberg, and T. Schneider (2011), Sources of variations in total column carbon dioxide, *Atmos. Chem. Phys.*, *11*, doi:10.5194/acp-11-3581-2011.

Lewis, S. L., P. M. Brando, O. L. Phillips, G. M. F. van der Heijden, and D. Nepstad (2011), The 2010 Amazon drought, *Science*, *331*, doi:10.1126/science.1200807.

Malhi, Y., J. T. Roberts, R. A. Betts, T. J. Killeen, W. Li, and C. A. Nobre (2009), Exploring the likelihood and mechanism of a climate-change-induced dieback of the Amazon rainforest, *P. Nat. Acad. Sci. USA*, *106*, 20610–20615.

Marengo, J. A., C. A. Nobre, J. Tomasella, M. D. Oyama, G. S. de Oliveira, R. de Oliveira, H. Camargo, L. M. Alves, and I. F. Brown (2008), The drought of Amazonia in 2005, *J. Climate*, *21*, 495.

Nassar, R., et al. (2010), Modeling global atmospheric CO2 with improved emission inventories and CO2 production from the oxidation of other carbon species, *Geosci. Model Dev.*, *3*, 689–716.

O'Dell, C. W., et al. (2012), The ACOS CO2 retrieval algorithm - Part 1: Description and validation against synthetic observations, *Atmos. Meas. Tech.*, *5*, 99–121.

Osterman, G., E. Martinez, A. Elderling, and C. Avis (2011), ACOS Level 2 Standard Product Data User's Guide, v2.9, retrieved from http://oco.jpl.nasa.gov/ocodatacenter/

Phillips, O. L., et al. (2009), Drought sensitivity of the Amazon rainforest, *Science*, *323*, 1344–1347.

Stephens, B. B., et al. (2007), Weak northern and strong tropical land carbon uptake from vertical profiles of atmospheric CO2, *Science*, *316*, 1732. doi:10.1126/science.1137004.

Vourlitis, G. L., N. P. Filho, M. M. S. Hayashi, J. de S. Nogueira, F. Raiter, W. Hoegel, and J. H. Campelo Jr. (2004), Effects of meteorological variations on the CO2 exchange of a Brazilian transitional tropical forest, *Ecol. Appl.*, *14*(4) Supplement, S89–S100.

Watanabe, H., A. Yuki, K. Hayashi, F. Kawazoe, N. Kikuchi, F. Takahashi, T. Matsunaga, and T. Yokota (2010), GOSAT higher level product status 1.5 year after the launch, *Proc. SPIE*, *7826*, 782606, doi:10.1117/12.898391.

Wunch, D., et al. (2011), A method for evaluating bias in global measurements of CO2 total columns from space, *Atmos. Chem. Phys.*, *11*, 12317–12337, doi:10.5194/acp-11-12317-2011.

Yoshida, Y., et al. (2011), Retrieval algorithm for CO2 and CH4 column abundances from short-wavelength infrared spectral observations by the Greenhouse gases observing satellite, *Atmos. Meas. Tech.*, *4*, 717–734, doi:10.5194/amt-4-717-2011.